

Magnetocaloric Effect in Amorphous and Partially Crystallized $\text{Fe}_{80}\text{Zr}_7\text{Cr}_6\text{Nb}_2\text{Cu}_1\text{B}_4$ Alloy

A. ŁUKIEWSKA^{a,*}, J. OLSZEWSKI^a, M. HASIAK^b AND P. GEĘBARA^a

^aCzęstochowa University of Technology, Institute of Physics, Armii Krajowej 19, 42-200 Częstochowa, Poland

^bWrocław University of Science and Technology, Smoluchowskiego 25, 50-370 Wrocław, Poland

In the present work the microstructure and thermomagnetic properties of $\text{Fe}_{80}\text{Zr}_7\text{Cr}_6\text{Nb}_2\text{Cu}_1\text{B}_4$ ribbon in the as-quenched state and after the accumulative annealing in the temperature range 600–800 K for 10 min were studied using Mössbauer spectroscopy and vibrating sample magnetometry. The second order phase transition from ferro- to paramagnetic state is observed. The Curie temperature T_C defined as inflection point on the magnetization versus temperature curve recorded on zero-field cooled mode equals 262.5 K for the as-quenched material. With increasing the annealing temperature increase of T_C is observed. The maximum value of the magnetic entropy change ($-\Delta S$) observed in the vicinity of the Curie point is equal to 0.85 J/(kg K) for the alloy in the as-quenched state. Moreover, for the samples annealed up to 750 K for 10 min the low intensity maximum at about 190 K related to the supplementary magnetic phase is observed. The presence of this phase was confirmed as additional component visible on hyperfine field distributions of Mössbauer spectra.

DOI: [10.12693/APhysPolA.133.676](https://doi.org/10.12693/APhysPolA.133.676)

PACS/topics: 65.60.+a, 75.50.Kj, 75.50.Bb, 75.30.Sg

1. Introduction

Amorphous metallic materials are characterized by unique mechanical, electrical, corrosion resistance and magnetic properties [1-4]. Some of them are very soft magnetic materials and their Curie temperature T_C could be easily tuned by the change of the chemical composition or/and proper heat treatment [5]. It allows to produce materials with T_C near room temperature which could be used as an active magnetic regenerator in magnetic refrigerator [6].

The aim of the present work is to study the structure and thermomagnetic properties (especially magnetic entropy change) of the $\text{Fe}_{80}\text{Zr}_7\text{Cr}_6\text{Nb}_2\text{Cu}_1\text{B}_4$ alloy fabricated in the form of ribbon. The investigation was carried out for determining its suitability for magnetic refrigeration.

2. Experimental procedure

The $\text{Fe}_{80}\text{Zr}_7\text{Cr}_6\text{Nb}_2\text{Cu}_1\text{B}_4$ alloy was prepared by arc melting under a protective argon atmosphere using high purity elements. Obtained ingot was remelted several times in order to achieve a good homogeneity. The amorphous ribbon 3 mm wide and 20 μm thick was produced by a single roller melt-spinning technique.

The microstructure of the investigated sample was studied using Bruker D8 Advanced X-ray diffractometer with $\text{CuK}\alpha$ radiation and conventional Mössbauer spectrometer with $^{57}\text{Co}(\text{Rh})$ radioactive source of 25 mCi activity. From transmission Mössbauer spectra analysis,

the average value of the quadrupole splitting QS , hyperfine field distributions $P(B)$ and phase composition of the samples in the as-quenched state and after annealing were determined by a Normos package according to the procedure developed in [7].

The magnetization measurements as a function of temperature (temperature range 50–400 K) and external magnetic field (up to 1 T) were carried out by the vibrating sample magnetometer (VSM) VersaLab system (Quantum Design). Magnetocaloric effect, studied as magnetic entropy change according to the Maxwell formula [8], was calculated basing on isothermal magnetization versus magnetic field.

To compare more precisely obtained results all investigations were carried out for the same piece of sample. Therefore, measurements were performed for as-quenched amorphous precursor and after the accumulative heat treatment at 600 K and then 700 K, 750 K and 800 K for 10 min. The conditions of the annealing were chosen according to the Differential Scanning Calorimetry (DSC) measurements (NETSCH STA 449F1 Jupiter) set at the heating rate of 10 K/min.

3. Results and discussion

Figure 1 shows the temperature dependence of heat flow for the as-quenched $\text{Fe}_{80}\text{Zr}_7\text{Cr}_6\text{Nb}_2\text{Cu}_1\text{B}_4$ alloy recorded with the help of Differential scanning calorimetry. It is seen that primary crystallization temperature is equal to 810 K. In diffraction patterns recorded for the $\text{Fe}_{80}\text{Zr}_7\text{Cr}_6\text{Nb}_2\text{Cu}_1\text{B}_4$ samples in the as-quenched state and after the annealing for 10 min at 600 K and then 700 K and 750 K only a broad halo, characteristic of amorphous materials, is observed. As an example, in Fig. 2a the X-ray diffraction pattern of the sample annealed at 600 K and then 700 K and 750 K is shown.

*corresponding author; e-mail: aluk@wip.pcz.pl

Mössbauer spectrum for this sample is present in Fig. 3a. Similar Mössbauer spectra measured at room temperature were obtained for samples in the asquenched state and after the accumulative annealing at 600 K and then 700 K [9]. These spectra are characteristic of amorphous paramagnets and have a form of asymmetric broad doublets. Further annealing at 800 K for 10 min leads to the partial crystallization of the investigated alloy. In X-ray diffraction pattern for $Fe_{80}Zr_7Cr_6Nb_2Cu_1B_4$ alloy after the annealing at 800 K for 10 min additional sharp peaks appear which correspond to the crystalline phases (Fig. 2b). It was also confirmed by Mössbauer studies (Fig. 3e). This Mössbauer spectrum, characteristic of paramagnetic partially crystalline material, was decomposed into three components corresponding to the amorphous matrix, interfacial zone and crystalline phase.

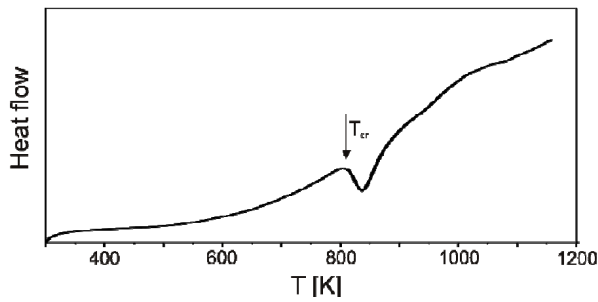


Fig. 1. DSC curve for $Fe_{80}Zr_7Cr_6Nb_2Cu_1B_4$ alloy. The arrow indicates the primary crystallization temperature (T_{cr}).

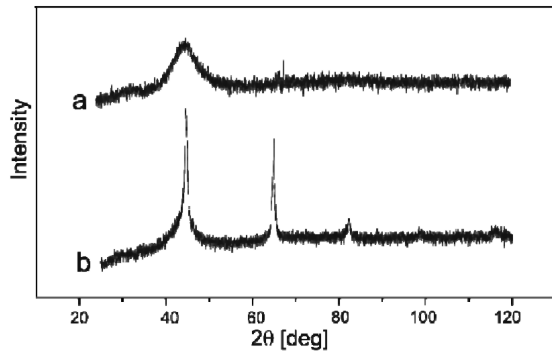


Fig. 2. X-ray diffraction patterns for $Fe_{80}Zr_7Cr_6Nb_2Cu_1B_4$ alloy after the accumulative heat treatment for 10 min at 600 K and then 700 K and 750 K (a) and 800 K (b).

The Curie temperatures obtained with numerically calculated derivatives from $\sigma(T)$ curves (Fig. 4) are presented in Table I. As it is shown in this table, the Curie temperature decreases after annealing at 600 K and slightly increases after the next stage of the heat treatment. Similar tendency is observed for average values of QS collected in Table 2. This behaviour is characteristic of materials exhibiting the invar effect [10].

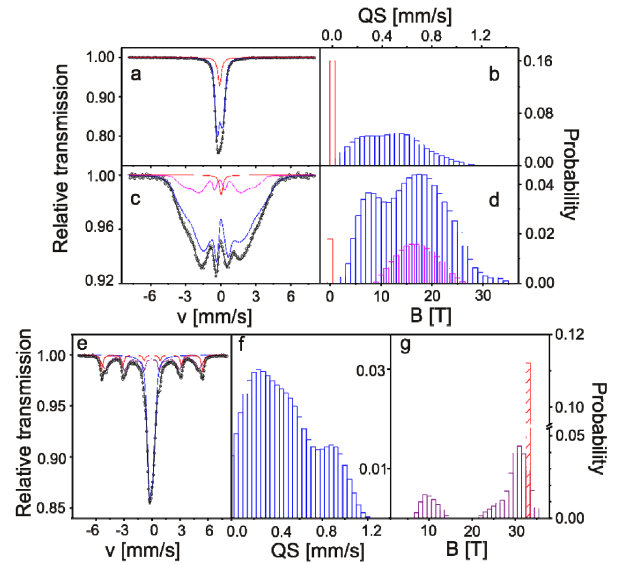


Fig. 3. Transmission Mössbauer spectra (a,c,e) measured at room temperature (a,e) and at liquid nitrogen (c), corresponding quadrupole splitting distributions (b, f) and hyperfine field distributions (d, g) for $Fe_{80}Zr_7Cr_6Nb_2Cu_1B_4$ alloy after the accumulative heat treatment for 10 min at 600 K and then at 700 K and 750 K (a,b,c,d) [9] and 800 K (e,f,g).

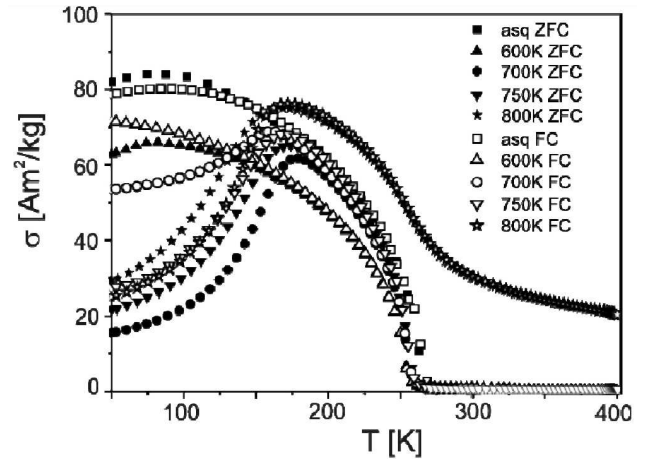


Fig. 4. The specific magnetization as a function of temperature measured at the magnetizing field induction of 5 mT after zero-field cooling (ZFC) and field cooling (FC) mode for $Fe_{80}Zr_7Cr_6Nb_2Cu_1B_4$ alloy.

The amount of heat transferred between the hot and cold reservoirs of a thermodynamic cycle, RCP was calculated from the formula:

$$RCP = (-\Delta S)_{\max} \delta T,$$

where δT is full width at half maximum of the $(-\Delta S)$ versus T curves [11].

In Fig. 5 σ^2 versus $\mu_0 H / \sigma$ i.e. the Arrott plots are depicted. In the present case, the slopes remain positive, indicating that the phase transition (from ferromag-

TABLE I

The Curie temperature T_C , the maximum magnetic entropy change $-\Delta S_{\max}$, the temperature of the maximum entropy change T_p and relative cooling power RCP of the major peak for investigated $\text{Fe}_{80}\text{Zr}_7\text{Cr}_6\text{Nb}_2\text{Cu}_1\text{B}_4$ alloy in the as-quenched state and after the accumulative annealing for 10 min at 600 K and then 700, 750, and 800 K.

Heat treatment	T_C [K]	$-\Delta S_{\max}$ [J/(kg K)]	T_p [K]	RCP [J/kg]
as-quenched	262.5	0.85	263	62
600 K	253.0	0.69	252	48
700 K	256.0	0.83	255	57
750 K	258.0	0.54	256	40
800 K	259.0	0.33	260	38

TABLE II

The average value of the quadrupole splitting distribution QS and its standard deviation $\langle QS \rangle$, isomer shift of the single line IS_{SL} and its relative intensity I_{SL} of $\text{Fe}_{80}\text{Zr}_7\text{Nb}_2\text{Cu}_1\text{B}_4$ alloy in the as-quenched state and after the accumulative heat treatment for 10 min at 600 K and then 700 and 750 K.

Heat treatment	QS [mm/s]	$\langle QS \rangle$ [mm/s]	I_{SL}	IS_{SL} [mm/s]
as-quenched	0.482	0.256	0.14	-0.027
600 K	0.478	0.249	0.14	-0.111
700 K	0.482	0.246	0.18	-0.101
750 K	0.482	0.250	0.16	-0.099

netic to paramagnetic state) is of the second order [12]. For the investigated alloy using the Maxwell thermodynamic relation the isothermal magnetic entropy changes ($-\Delta S$) was calculated according to the procedure described in [13]. The magnetic entropy changes as a function of temperature for the maximum magnetizing field induction $B_m = 1$ T are shown in Fig. 6.

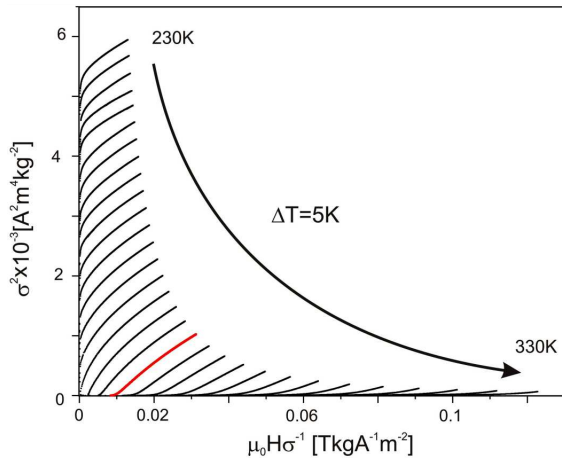


Fig. 5. Exemplary set of Arrott plots for $\text{Fe}_{80}\text{Zr}_7\text{Cr}_6\text{Nb}_2\text{Cu}_1\text{B}_4$ alloy after the accumulative heat treatment for 10 min at 600 K and then at 700 and 750 K.

The magnetic entropy change achieves the highest value $-\Delta S_{\max}$ for the investigated alloy in the as-quenched state and decreases after the annealing at 750 K and then at 800 K. The temperature of the maximum entropy change T_p is observed near the Curie point and shifts toward temperatures scale like the T_C . It is worth noticing that the second, low intensity maximum, near 180 K is also visible. Furthermore, in $\sigma(T)$ curves the bifurcation between ZFC and FC results in this temperature range disappears (Fig. 4).

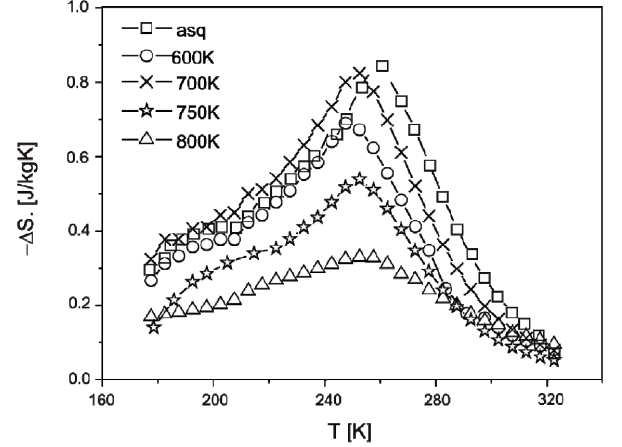


Fig. 6. The magnetic entropy change versus temperature of $\text{Fe}_{80}\text{Zr}_7\text{Cr}_6\text{Nb}_2\text{Cu}_1\text{B}_4$ alloy in the as-quenched state and after the accumulative annealing for 10 min at 600 K and then 700, 750 and 800 K.

This maximum on $\Delta S(T)$ curves observed for samples annealed up to 750 K is related to low intensity components on $P(B)$ and $P(QS)$ distributions. The hyperfine field distribution obtained from the Mössbauer spectrum, collected at the liquid nitrogen temperature, consists of two continuous components with average hyperfine field $B_1 = 15.8$ T, $B_2 = 17.0$ T and relative intensities $I_1 = 0.82$, $I_2 = 0.16$, respectively. The similar components, with the same intensities, we distinguished in the quadrupole splitting distribution for the spectrum measured at room temperature (Fig. 3b) and one of them (the single line for $QS=0$) is ascribed to Fe sites with the cubic symmetry of atoms arrangement in the nearest neighbourhood [10].

4. Conclusions

The Curie temperature for the $\text{Fe}_{80}\text{Cr}_6\text{Zr}_7\text{Nb}_2\text{Cu}_1\text{B}_4$ alloy in the as-quenched state equals to 263 K. After annealing at 600 K the Curie temperature drops down and then monotonically increases for the investigated samples annealed up to 800 K. This behaviour is connected to the invar effect.

For the investigated $\text{Fe}_{80}\text{Zr}_7\text{Cr}_6\text{Nb}_2\text{Cu}_1\text{B}_4$ alloy the highest value of the magnetic entropy change of 0.85 J/(kg K) is observed in the as-quenched state and occurs in the vicinity of the Curie point.

The additional maximum in $\Delta S(T)$ curve, visible at low temperatures, indicates the biphasic structure of the material. Such structure consists of areas with different concentration of Fe atoms, what is visible as low and high field components on hyperfine field distributions of Mössbauer spectra.

References

- [1] M.E. McHenry, M.A. Willard, D.E. Laughlin, *Progress in Materials Science* **44**, 291 (1999).
- [2] J.M. Barandiaran, P. Gorria, I. Orue et al., *J Phys Condens Matter* **9**, 5671 (1997).
- [3] W. Pilarczyk, *Cryst. Res. Technol.* **50**, 700 (2015).
- [4] R. Babilas, A. Radoń, P. Gębara, *Acta Phys. Pol. A* **131**, 726 (2017).
- [5] L.F. Kiss, T. Kemeny, V. Franco, A. Conde, *J. Alloys Comp.* **622**, 756 (2015).
- [6] K.A. Gschneidner, V.K. Pecharski, A.O. Tsokol, *Rep.Prog. Phys.* **68**, 1479 (2005).
- [7] R. A. Brand, *Phys. Res.* **B28**, 398 (1987).
- [8] V.K. Pecharski, K. A. Gschneidner, *J. Mag. Mag.Mater.*, **200**, 46 (1999).
- [9] A. Łukiewska, *Nukleonika* **62**, 135 (2017).
- [10] J. Olszewski, *Hyperfine Interactions.* **131**, 83 (2000).
- [11] V. Chaudhary, R.V. Ramanujan, *IEEE Magn. Lett.* **6** (2015).
- [12] X.C. Zhong, H. C. Tian, S. S. Wang, Z. W. Liu, Z. G. Zheng, D. C. Zeng, *J. Alloys Comp.* **633**, 188 (2015).
- [13] J. Świerczek, *J. Mag. Mag. Mater.* **322**, 2696 (2010).